Chinese Science Bulletin

Prostate cancer targeted MRI nanoprobe based on superparamagnetic iron oxide and copolymer of poly(ethylene glycol) and polyethyleneimin

ZHOU JianHua[1*], HUANG Lü[2*], WANG WeiWei[2], PANG Jun[1], ZOU Yang[3], SHUAI XinTao[2†] & GAO Xin[1†]

[1] Department of Urology, Third Affiliated Hospital of Sun Yat-sen University, Guangzhou 510630, China;
[2] BME Center, School of Chemistry and Chemical Engineering, Sun Yat-sen University, Guangzhou 510275, China;
[3] Department of Radiology, Third Affiliated Hospital of Sun Yat-sen University, Guangzhou 510630, China

Methoxyl poly (ethylene glycol) (mPEG-OH) was successfully grafted onto branched polyethyleneimine (hy-PEI) to yield a water soluble graft copolymer mPEG-g-PEI. This copolymer may package superparamagnetic iron oxide (SPIO) by ligand exchange. The SPIO weight percentage in the polymer coated nanoparticles was determined to be 55%, the size and zeta potential of nanoparticles was 50 nm and 12 mV respectively. Antibody fixation onto the complex (mPEI-g-PEG-SPIO) surface layer was achieved by activated single chain monoclonal antibody against prostate stem cell antigen (PSCA). Our study showed that the single chain antibody functionalized nanoprobe ($scAb_{PSCA}$-PEI-g-PEG-SPIO) with a small size can specifically enter the prostate cancer cells, decreasing MRI T2-weighted signal intensity of prostate cancer cells to 44.76%. Our results revealed that the potential of this magnetic nanoparticulate system promised as a novel MRI nanoprobe for early diagnosis of prostate cancer (PCa).

PEG-grafted-hyperbranched-PEI (PEG-g-PEI), prostate cancer (PCa), prostate stem cell antigen (PSCA), superparamagnetic iron oxide nanoparticles (SPIO), magnetic resonance imaging (MRI)

Prostate cancer (PCa) is the most frequently diagnosed cancer in men in the western countries, and is expected to rise up to more than 100000 new cases per year in 2020[1]. Because the tumor has often extended beyond the confinement of the prostate capsule as advanced PCa at the time of diagnosis, patients often lose the chances of radical prostatectomy. Although being treated by operation or androgen deprivation, advanced PCas often develop to metastatic PCas and eventually develop into hormone-refractory prostate cancer (HRPC) within a few years. Systemic treatment combined with effective palliative chemotherapy only improves median survival time from an average of about 12 months to 17—18 months in HRPC patients[2]. Due to the lack of effective therapy for advanced PCa, diagnosis of early PCa is of great significance. However, various kinds of diagnostic methods including prostate specific antigen (PSA) value of blood serum, digital rectal examination (DRE), transrectal ultrasound (TRUS), and magnetic resonance imaging (MRI) used by urologists now can not efficiently detect early stage PCa[3]. In addition, although prostatic biopsy is regarded as a diagnostic golden standard for PCa, and more cores biopsy will increase its final diagnosis, it would hurt other organs by mistake or increase the risk of complication[4]. On the other hand, results of biopsy guidance by TRUS have shown a high false negative rate of approximately 11%[5,6]. MRI, a powerful method for noninvasive three-dimensional imaging of cells and human bodies, is an approach to detect the lesions of PCa and has the advantages of high distin-

Received November 24, 2008; accepted March 2, 2009
doi: 10.1007/s11434-009-0256-6
†Corresponding authors (email: Xin.Gao.zsu@gmail.com , shuaixt@mail.sysu.edu.cn)
*Contributed equally to this work
Supported by the National Natural Science Foundation of China (Grant Nos. 30772178, 50673103), Natural Science Foundation of Guangdong Province (Grant Nos. 7117362, 7003703) and Key Clinical Program of Ministry of Health Foundation of China

Citation: Zhou J H, Huang L, Wang W W, et al. Prostate cancer targeted MRI nanoprobe based on superparamagnetic iron oxide and copolymer of poly(ethylene glycol) and polyethyleneimin. Chinese Sci Bull, 2009, 54: 3137—3146, doi: 10.1007/s11434-009-0256-6

guishing ability of soft tissue, good imaging sensitivity, data repeatability and the potential to improve the identification of PCa among the various prostate-imaging modalities. Molecular imaging of target cells can be achieved by using MRI probes that can specifically bind to the target cells [7,8]. One area in this rapidly advancing field is the development of novel MRI contrast agents, such as smart agents that can produce a contrast in response to small molecules or biomolecular markers in cells or human bodies. Among the smart MRI contrasts, superparamagnetic iron oxide (SPIO) has attracted great attention among many researchers[9]. SPIO is nano-molecular probe with good biocompatibility, magnetic resonance signal sensitivity and excellent MRI T2 contrast compared with other MRI contrast agents. Modifying SPIO surface with different polymers such as citric[10], oleic acid[11], dextran[12], poly-epsilon caprolactone[13], silica/silanes[14], PEGs[15], poly-glutamic benzyl acid (PBLG)[16], polyethyleneimine (PEI)[17], protein[18], monoclonal antibodies (mAbs)[19], trypsin[20], and DNA[21] can significantly improve the stability of SPIO in the physical environment, extend circulation time and improve targeting efficiency of the transportation. The modified SPIO as MRI probe has been widely applied to various cells[22]. Loading the mAbs which can target cancer cells and SPIO to the same vector system will result in MRI T2 contrast agents with cancer cells specificity and consequently improve the sensitivity of tumor MRI diagnosis.

Prostate stem cell antigen (PSCA) is a PCa cell surface GPI-anchored protein, which does not exist in the blood and is highly prostate-specific. Normal prostate substrate cells express only low-level of PSCA, and exocrine cells and stromal cells hardly express PSCA. High-level prostatic intraepithelial neoplasia, both androgen-dependent and androgen-independent PCa, show a high expression of PSCA and metastatic PCa all show very strong expression[23]. The PSCA expression level between PCa tissues and normal prostatic tissues has significant statistical difference. Both clinical stages and cell grades of PCa are not statistically correlated to the PSCA expression level [24]. The restrictive expression of PSCA in normal tissues and the significant cell-surface expression in tumors strongly support the idea that PSCA may be a potent target for tumor diagnosis and therapy [25]. Therefore, we select PSCA as a target antigen for targeting molecular MRI of PCa.

In the present research, polyethylene glycol (PEG)-modified PEI packaging SPIO was connected with a single chain mAb ($scAb_{PSCA}$) to target PSCA. The cytotoxicity, size and zeta potential of Ab_{PSCA}-PEG-g-PEI-SPIO nanocomplexes was determined. PCa cell culture in the presence of the nano-probes was conducted to investigate the cell uptake efficiency of PCa-targeted magnetic nanoparticles by looking into the change in magnetic resonance signal intensity as well as Prussian blue staining. The current study aims to lay a foundation for early diagnosis of PCa with PCa-specific and sensitive MRI molecular contrast agent.

1 Materials and methods

1.1 Reagents

Monomethoxy polyethylene glycol (mPEG-OH) (MWCO = 2 kD), N-hydroxysuccinimide (NHS), N, N′-carbonyldiimidazole (CDI) 2-mercaptoethylamine were purchased from Sigma-Aldrich. N-methoxycarbonyl-maleimide was purchased from Fluka. Hyperbranched polyethyleneimine (hy-PEI) (MWCO=25 kD) was purchased from BASF. Dicyclohexylcarbodiimide (DCC) and succinic anhydride were purchased from Sinopharm Chemical Reagent Limited Company. Ethylenediaminetetraaceticacid (EDTA) was purchased from Guangzhou Chemical Reagent Factory. Tetrahydrofuran (THF) and chloroform ($CHCl_3$) were dried over CaH_2, and distilled before use. Phosphate Buffered Saline (PBS pH 7.4) was prepared. SPIO measuring 6 nm in averaged diameter was synthesized following the method reported by Sun et al.[26]. α-Hydroxy-ω-amino-poly (ethylene glycol) (HO-PEG-NH_2) (M_n = 3600, M_w/M_n = 1.3) was prepared according to a report by Tromsdorf et al.[27]. Cell culture media and fetal bovine serum (FBS) were purchased from Invitrogen Corporation (Carlsbad, CA, USA). Fluorescent staining agents 4′, 6-diamidino-2-phenylindole (DAPI), were purchased from Molecular Probes, Inc. (Eugene, USA. PSCA mAb (7F5) were purchased from Santa Cruz Biotechnology, INC (California, USA). Gelatin was purchased from Whiga Technology Co., Ltd. (Guangzhou, China).

1.2 Instruments

Varian INOVA 500NB superconducting NMR analysis was used to identify the chemical structure of products. The encapsulation efficiency of SPIO in nanoparticles was determined using a polarized Zeeman Atomic Absorption Spectrophotometer (Model: Z-2000 series).

Nanoparticle zeta potential was determined with Zeta-Plus instrument (Brookhaven, NY, USA) at position of 45° angle at 25℃. Size was determined on the same instrument at 25℃ and scattering light was detected at 90° angle. CLSM observations were carried out using a Zeiss LSM 510 META microscope (Carl Zeiss Co., Ltd., Gottingen, Germany). Carl Zeiss Aviox-1 inverted fluorescence microscope (Carl Zeiss Co., Ltd., Gottingen, Germany). MRI examinations were conducted on a GE (Signal Twin Speed Excite II) 1.5-T scanner employing a 77 mT/m (150 mT/m ms) gradient system at room temperature. Cytotoxicity assay was recorded on a Tecan Infinite F200 Multimode plate reader and the absorbance at 570 nm.

1.3 Cell Culture

The human PCa cell line PC3, PC3M and NIH3T3 were used for transfection. PC3 and PC3M were ordered from American Type Culture Collection (ATCC, Manassas, VA). Cells were grown in high glucose Dulbecco's Modified Eagle Medium (DMEM) (GIBCO, Grand Island, New York, USA), supplemented with 10% fetal bovine serum at 37℃ under 5% CO_2. For experimentation, PC3M, PC3 and NIH3T3 cells were seeded onto 6-well plates at a density of 5.0×10^5 cells/well under the aforementioned conditions for 1 day before addition of complexes, then the cells were subject to Prussian staining and MRI scan. 1.0×10^5 cells/well were plated in 12-well plates for immunofluorescence.

1.4 Experiment

(i) Synthesis of mPEG-g-PEI. 4.0 g of mPEG-OH (MWCO = 2 kD) in a 100 mL flask was vacuum-dried at 60℃ for 5 h, then 30 mL of anhydrous THF was added to dissolve the polymer under a dry argon atmosphere. And 2.27 g of CDI was dissolved in 20 mL of anhydrous THF. The mPEG-OH solution was added dropwise to the CDI solution and then the mixture was stirred for 12 h. Excessive CDI was reacted by injecting 0.216 mL distilled water and the reaction continued for about 0.5 h. The mixture was evaporated by revolving evaporator. The residues were precipitated in cool diethyl ether and the white powdery product was obtained by filtration and further purified by the elimination of ether on reduced pressure.

Then 3.0 g of hy-PEI (M_n = 3.6 kD) and 2.4 g of the above-mentioned white powdery solid were dissolved in 10 mL $CHCl_3$ and completely mixed by stirring overnight. The mixture was precipitated in cool diethyl ether for 3 times. The solid was collected by filtration and vacuum-dried to a constant weight at room temperature. Yield: 70%. The reaction was shown in Figure 1.

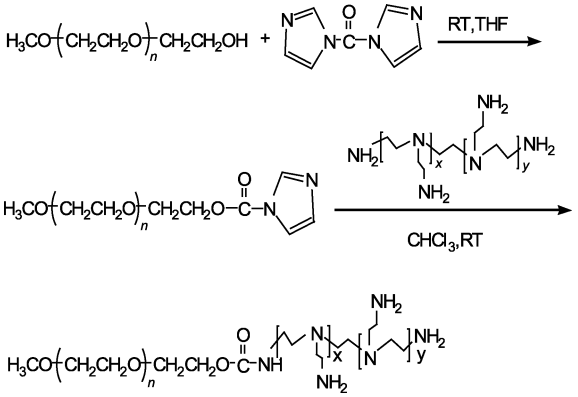

Figure 1 Synthesis of mPEG-g-PEI.

(ii) SPIO Encapsulation with mPEG-g-PEI. PEG-g-PEI coated SPIO nanoparticles (mPEI-g-PEG-SPIO) was prepared by a "ligand exchange" method (Figure 2) as reported by Tromsdorf et al.[27].

450 mg of PEG-g-PEI and 30 mg of SPIO was dissolved in 5 mL of $CHCl_3$. The reaction mixture was stirred overnight at room temperature, and then precipitated into about 10 mL of hexane. The precipitate was shaken for 3 h and removed the supernatant using a pipettor. This operation was repeated for 3 times and the organic solvents were evaporated. The product was dispersed into double distilled water under sonication, centrifugated at the speed of 12000 r/min for 1.5 h, and then the supernatant was filtered through a 220 nm membrane to remove large aggregates. The product was kept at 4℃ for use. The encapsulation efficiency of SPIO in nanoparticles was determined using a polarized Zeeman Atomic Absorption Spectrophotometer (Model: Z-2000 series). In details, preweighed nanoparticle was dispersed in 1 $mol\cdot L^{-1}$ HCl aqueous solution to allow a complete dissolution of SPIO. The iron concentration was determined by measuring the specific Fe absorption around 248 nm. A pre-established calibration curve was used for the calculation of the iron concentration. The SPIO loading content in nanoparticles was calculated as the ratio of iron oxide over the total weight of the nanoparticle sample.

(iii) Synthesis of α-carboxyl-ω-maleimide-poly (ethylene glycol) (mal-PEG-COOH). Mal-PEG-OH was synthesized according to a report by Shen et al.[28]. 3.0 g

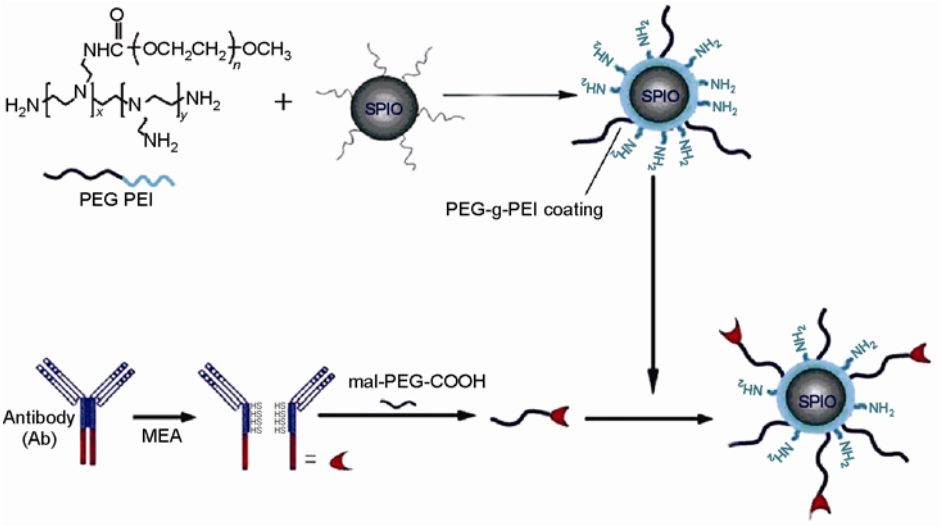

Figure 2 Synthesis of mPEG-g-PEI-SPIO and scAb-PEG-g-PEI-SPIO.

of HO-PEG-NH_2 (M_n=3.6 kD) was dissolved in 15 mL of a saturated aqueous solution of $NaHCO_3$, and the mixture was cooled to 0℃ by an ice/salt bath. After 0.42 g of N-methoxycarbonylmaleimide was added, the solution was stirred for 10 minutes. Subsequently, 30 mL of water was added and the solution was stirred for another 45 minutes. The pH value of the above solution was adjusted to 3.0 with sulfuric acid (0.5 mol·L^{-1}), and then the mixture was extracted with CH_2Cl_2 for 3 times and dried with Na_2SO_4. After filtering off Na_2SO_4, the solution was precipitated into large amount of cold diethyl ether. The precipitate was collected by filtration and vacuum-dried to a constant weight at room temperature. Finally, a white powdery solid was obtained. Then, according to a report by Shuai et al.[29], mal-PEG- COOH was synthesized. Typically, 300 mg of the above- mentioned white powdery solid vacuum-dried for 5h at room temperature was dissolved in 20 mL dried $CHCl_3$ by vigorous stirring. Subsequently, 50 mg of succinic anhydride was added to the solution and the mixture under a dry argon atmosphere was stirred at 70℃ for 48 h. The mixture was subject to rotary evaporation to remove most part of $CHCl_3$ and the residues were precipitated in large amount of cold diethyl ether. The white powdery product was collected by filtration and lyophilization. The reaction was shown in Figure 3.

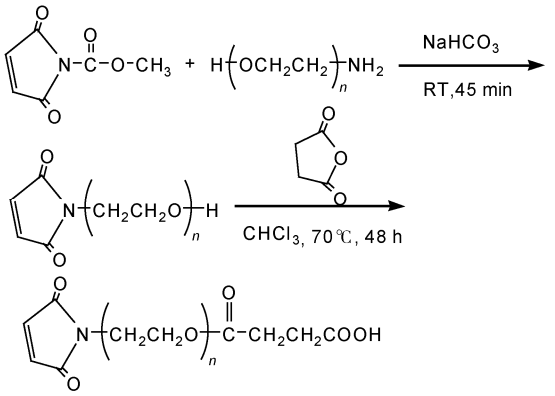

Figure 3 Synthesis of mal-PEG-COOH.

(iv) Synthesis of Ab_{PSCA} single chain monoclonal antibody conjugated magnetic nanoparticle ($scAb_{PSCA}$-PEG-g-PEI-SPIO). The synthetic process of $scAb_{PSCA}$-PEG-g-PEI-SPIO was outlined in Figure 2. The single chain monoclonal antibody (scAb) bearing free sulfhydryl groups were pre pared for conjugation to nanoparticles according to the literature report[30]. 50 μL of Ab_{PSCA} in aqueous solution (0.2 mg/mL, antibody molecular weight: 29 kD) was dissolved in 10 μL EDTA aqueous solution (0.5 mol·L^{-1}). 2-Mercapto ethylamine (60 mg) and 10 μL of 0.5 mol·L^{-1} EDTA aqueous solution was added into PBS (500 μL) and then mixed with the antibody solution. After incubation for 90 min at 37℃, the obtained scAb solution was purified by ultrafiltration in an Amicon cell (regenerated cellulose membrane, MWCO = 5 kD) following 3 times wash with PBS (pH 7.4, each 500 μL containing 10 μL of 0.5 mol·L^{-1} EDTA solution). 10 μg mal-PEG-COOH dissolved in 10 μL PBS containing 10 μL of 0.5 mol·L^{-1} EDTA solution was added to the scAb solution and then incubated overnight at 4℃. The resultant solution containing scAb functionalized PEG ($scAb_{PSCA}$-PEG-COOH) was washed 3 times

with PBS (pH 7.4) following ultrafiltration in an Amicon cell (MWCO = 5 kD). Dicyclohexylcarbodiimide (DCC, 5 μg) and N-hydroxysuccinimide (NHS, 5 μg) were added to the purified solution, followed by addition of PEG-g- PEI-coated SPIO (10 μg). The solution was adjusted to 100 μL with PBS and incubated overnight at 4 ℃.

To determinate whether the Ab_{PSCA} has been successfully linked to PEG-g-PEI coated SPIO, the magnetic complexes were stained with anti-IgG antibody-FITC conjugate (Wuhan Boster Biological Technology, LTD., China) following the supplier's instructions. After centrifugation and discarding the supernatant, an appropriate amount of PBS was added to resuspend the magnetic nanoparticles. PC3M cells were incubated with the above solution for 20 min at 37℃, washed with PBS and then observed on a Carl Zeiss Aviox-1 inverted fluorescence microscope (Carl Zeiss Co., Ltd., Gottingen, Germany).

(v) Zeta potential and size measurements. Zeta-potential measurement of nanoparticles including $scAb_{PSCA}$-PEG-g-PEI-SPIO, mPEG-g-PEI-SPIO was carried out using a Zeta-Plus instrument (Brookhaven, NY, USA) at position of 45° angle at 25℃. The averaged values plus standard deviations were based on the data of three runs. Nanoparticle size was determined on the same instrument at 25℃. Scattering light was detected at 90° angle, and the sizes given were the means of three runs plus standard deviations.

(vi) Cytotoxicity assay *in vitro*. PC3 cells were seeded in 96-well plates at an initial density of 5000 cells/well in 0.2 mL of growth medium and incubated for 24 h prior to the addition of polymers. The growth medium was replaced by medium containing different amounts of polymers. After additional incubation for 24 h, the medium was changed to test cells cytotoxicity.

Using the WST-8 assay with Cell Counting Kit-8 (Dojindo, Kumamoto, Japan) as described in the manufacturer's manual[31], cytotoxicity *in vitro* of the polymers with or without SPIO encapsulation was evaluated. PEI, PEG-g-PEI, and PEG-g-PEI–SPIO were tested to assess cytotoxicity. After cells were incubated in the presence of polymers for 24 h, 100 μL medium containing 10 μL of WST-8 solution was added. The cells were further incubated for 4 h, and the absorbance at 570 nm was recorded on a Tecan Infinite F200 Multimode plate reader. All experiments were conducted in triplicates.

(vii) Confocal laser scanning microscopy (CLSM) experiment study on cellular uptake of nanoparticles. Cells were cultured for 24 h to confluence in order to observe fluorescence emission by CLSM. CLSM examination was conducted on a Lab-Tek glass chamber slide (Nalge Nunc International, Naperville, IN). The complexes were added in Fe concentrations of 40 μg/mL for 2 h at 37℃. After being washed 3 times in PBS, cells were fixed in 4% paraformaldehyde (10 min at 4°C), washed and blocked with 1% bovine serum albumin in PBS for 10 min at room temperature. Then the cells were incubated with FITC-labeled goat anti-mouse IgG diluted at 1:10 for 1 hour at 4℃.

To identify Ab_{PSCA}-PEG-g-PEI-SPIO location, cell nuclei were stained with DAPI. Samples were examined by CLSM using a Zeiss LSM 510 microscope (Zurich, Switzerland, lasers: He-Ne 543/633 nm, Ar 458/488/514 nm, Ti: Sapphire 700—900 nm) with a confocal plane of 100 nm. Z-sectioning was used for identification of complexes intracellular location. Image processing was performed on an IBM Graphics workstation using Zeiss LSM 510 software. For excitation of DAPI fluorescence, an Enterprise UV laser with an excitation wavelength of 358 nm was used. Excitation of FITC was performed using an argon laser with an excitation wavelength of 488 nm. CLSM observations were carried out using a Zeiss LSM 510 META microscope (Carl Zeiss Co., Ltd., Gottingen, Germany).

(viii) Prussian blue staining. PC3M cells were seeded in 12-well plates at a density of 1×10^5 cells per well. Nanoparticles mPEI-g-PEG-SPIO or $scAb_{PSCA}$-PEI-g-PEG-SPIO were diluted in PBS and then added to 12-well plates at a Fe concentration of 40 μg/mL per well. After incubation for 2 h at 37℃, cells were washed with fresh PBS, fixed with 4% paraformaldehyde solution for 10 min, washed again with PBS, and further incubated for 30 min at 37℃ with Prussian blue solution comprising equal volume of 2% aqueous solution of hydrochloric acid and 2% potassium ferrocyanide (II) trihydrate. After being washed three times with deionized water, cells were finally observed using a Zeiss microscope to evaluate the iron staining effect.

(ix) MRI scanning *in vitro*. PC3M cells, at a number of 5×10^5 cells per well, were incubated for 2 h in the presence of nanoparticles with or without Ab_{PSCA} attachment containing SPIO at a concentration of 40 μg/mL in DMEM media. The cells were washed three

times with PBS, collected by digesting with pancreatic enzyme, centrifugated at 1000 r/min for 5 min at room temperature, and resuspended with 2% gelatin (200 μL) for MRI scanning.

MRI examinations were conducted on a GE (Signal Twin Speed Excite II) 1.5-T scanner employing a 77 mT/m (150 mT/m ms) gradient system at room temperature. Samples were tested using SE pulse sequence of two different TE times with parameters: TR400ms, BW 20.8 kHz, 20×20FOV, 320×224 matrix, Slice thickness 3 mm, Space 1 mm, 2 NEX, 3:02 min Scan Time, 8HRBRAIN coil, TE1 of 15 ms and TE2 of 45 ms. T_2-weighted image and the values of T_2-weighted signal intensity were obtained, and the values of T_2 release time were calculated as

$$T_2 = (\mathrm{TE2}-\mathrm{TE1})/\ln(S_1/S_2),$$

according to the formula:

$$S(t) = S_0\exp(-\tau/T_2).$$

1.5 Statistical analysis

Data were presented as (mean ± SD). Statistical differences were considered to be significant at a P-value less than 0.05 as determined by a paired Student's t test using SPSSv11.5 (SPSS Inc., Chicago, IL, USA).

2 Result and discussion

Using polymeric nano-probes for early disease diagnosis has immerged as a novel medical practice at present. This type of probes has two prominent characteristics: (i) Unique nano-size (10—100 nm) decreasing kidney excretion, endothelium network absorption and cytophagous identification, consequently extending circulation time in body. (ii) Specific passive targeting to cancer tissues having the features of abundant blood capillary, large gaps of blood vessel endotheliums, insufficient lymphatic vessel which let nanoparticles easily enter cancer tissues, and difficultly retaken up by lymphatic system into recirculating system. By these enhanced penetration and retention, the polymer nanoparticles obtained a passively targeted aggregation. In addition, receptor-mediated nanoparticle endocytosis introduced by the corresponding ligands has been proven to enhance the nanoparticle endocytosis in tumor cells, which also provides an effective way to avoid endocytosis in normal cells.

Developing diagnostic nanoprobe for cancer is a hot field in early disease diagnosis. The antibody targeting has a great deal of concern in lots of tumor cells as an active ligand targeting technology for its features of high specificity, high selectivity, powerful affinity and apparent biological effect. Antibody is composed of two same chains that can be broken into two single chains with the same trait of binding to its receptor. However, its volume and weight are diminished, and can enter cell more easily by endocytosis. PSCA, a protein of membrane antigen highly expressed on PCa, can bind to its monoclonal antibody and is a potential membrane protein of PCa for targeting diagnosis and therapy. The specific binding of single chain monoclonal PSCA antibody will offer an efficient MRI nano-SPIO probe for early PCa diagnosis.

2.1 Synthesis of mPEG-g-PEI-SPIO

PEI-g-PEG was synthesized by conjugating CDI activated PEG to PEI. 1H-NMR analysis of the dialyzed PEI-g-PEG revealed prominent chemical shifts of protons from PEG (—OCH_2CH_2—, 3.65 ppm (1 ppm = 10^{-6}); CH_3O—, 3.38 ppm) and PEI (—CH_2CH_2NH—, 2.5—2.9 ppm) respectively, indicating that PEG chains were successfully grafted onto PEI chains (Figure 4). mPEI-g-PEG-SPIO was synthesized successfully by "ligand exchange" method. By this approach the cationic copolymer PEI-g-PEG replaced the hydrophobic coating of oleic acid/oleylamine on the nanoparticle surface of SPIO measuring 6 nm. The SPIO weight percentage in the polymer coated nanoparticles was determined to be 55%. The dispersion of the obtained complex, mPEI-g-PEG-SPIO, is stable in water.

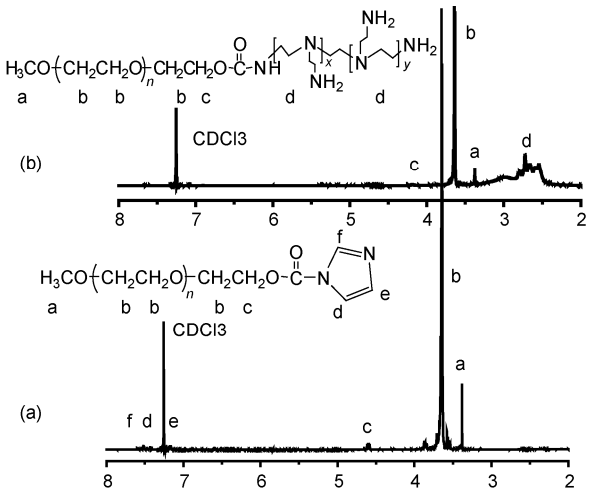

Figure 4 1H-NMR spectra of mPEG-CDI (a) and mPEG-g-PEI (b).

2.2 Zeta potential and size measurements

The nanoparticles with hydrophilic shells can be completely dispersed in aqueous physiological fluid *in vivo* and may be sent to the specific diseased sites by blood circulation. The particle size and zeta potential of $scAb_{PSCA}$-PEG-g-PEI-SPIO and mPEG-g-PEI-SPIO detected by the Zeta-Plus instrument are shown in Figure 5 and Table 1.

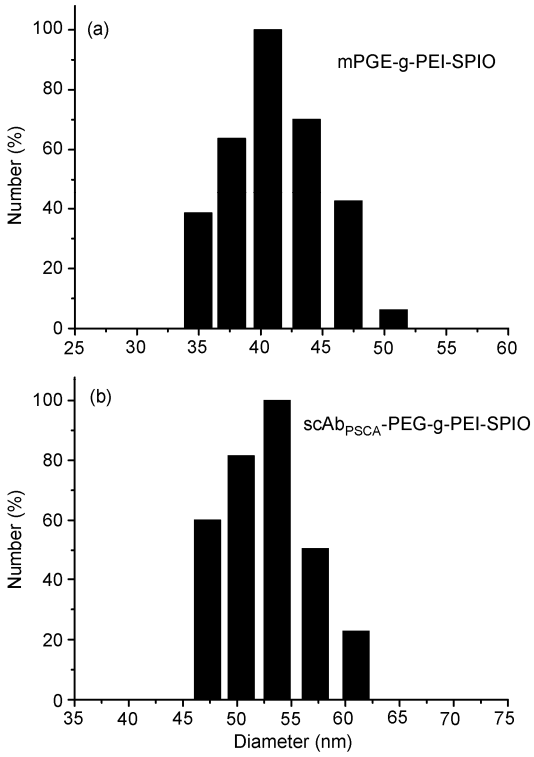

Figure 5 Size distribution of mPEG-g-PEI-SPIO and $scAb_{PSCA}$-PEG-g-PEI-SPIO nanoparticles.

Table 1 Zeta potential of mPEG-g-PEI-SPIO and $scAb_{PSCA}$-PEG-g-PEI-SPIO

	mPEG-g-PEI-SPIO	$scAb_{PSCA}$-PEG-g-PEI-SPIO
Zeta potential (mV)	28±3.77	10±1.23

The change of particle size and zeta potential upon antibody attachment was consistent with our expectation. On average, the particle size of mPEG-g-PEI-SPIO was (42 ± 3.2) nm and the surface zeta potential was about (28 ± 3.77) mV as detected at room temperature. After single-chain antibody attachment, the particle size of magnetic nanoparticles increased to (53 ± 1.2) nm, which was still an ideal size for application of transfection. The surface zeta potential of particles dramatically decreased to (10 ± 1.23) mV, apparently due to interaction between the scAb and positive mPEG-g-PEI-SPIO. The medium decrease of surface potential can make the nanoparticles keep good endocytosis and meanwhile reduce nonspecific cell absorption and cationic toxicity, i.e. the overall property of the nanoprobe can be improved in theory.

The relatively small particle size of these PCa targeted magnetic nanoparticles potentially enable them to have a long circulation time *in vivo*, which is essential for ideal cancer cell transfection in tumor sites.

2.3 Cytotoxicity analysis using wst-8 assay *in vitro*

WST-8 was utilized in the cytotoxicity assay. The PC3 cells were incubated with PEI, mPEG-g-PEI and mPEG-g-PEI-SPIO. Different concentrations of PEI were used in cytotoxicity assay *in vitro* (Figure 6). In all groups, cell viability was gradually decreased along with increase in PEI concentration. At the concentration of 0.1 μg/mL, 1 μg/mL, 5 μg/mL, 10 μg/mL, 50 μg/mL, 100 μg/mL, 500 μg/mL and 1000 μg/mL PEI, mPEG-g- PEI, mPEG-g-PEI-SPIO groups showed comparable decrease in cell viability. However, PEI group exhibited much more significant decrease in cell viability than other groups at concentrations above 100μg/mL due to its high cationic toxicity.

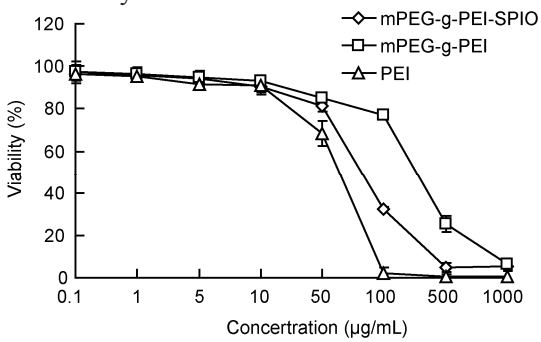

Figure 6 Cytotoxicity of nanoparticles in PC3 cells.

These results demonstrated that PEG modification of PEI had reduced the cytotoxicity of PEI by decreasing the vector zeta potential as detected in the zeta potential measurement. In addition, polymers linking to SPIO did not affect cytotoxicity of mPEG-g-PEI obviously. As a whole, PEI modified with mal-PEG and SPIO is much less toxic than the unmodified PEI.

2.4 CLSM study on cellular uptake of nanoprobes

We incubated the PC3M cells with targeting complexes and non-targeting complexes respectively, and then examined the cell uptake of nanoprobes by confocal laser scanning microscopy (Figure 7).

As shown in the microscopic images (Figure 7(b)),

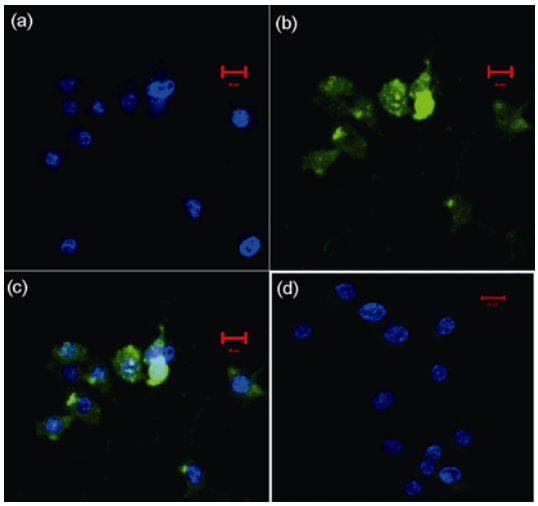

Figure 7 Laser confocal microscope images of PC3M cells after 2 h incubation with $scAb_{PSCA}$-PEG-g-PEI-SPIO ((a)－(c); (c) is an overlay of (a) and (b)) and PEG-g-PEI-SPIO (d) labeled with the second Ab, FITC-IgG (image magnification 400×). Images assignment in (a)－(d): blue: nucleus, green: FITC-IgG..

cells incubated with the targeting complexes showed stronger green fluorescence, whereas the cells incubated with non-targeting complexes only showed nucleic blue fluorescent stain (Figure 7(d)). This is a strong indication that the fluorescence-labeled $scAb_{PSCA}$-PEG-g-PEI-SPIO complex has efficient cell binding. These results suggested that PC3M cell binding of $scAb_{PSCA}$-PEG-g-PEI-SPIO complexes are associated with PSCA receptors on the PC3M cells surface, and the targeting ligand has potent effect on the cell uptake of nanoprobes.

2.5 Prussian blue staining

For Prussian blue staining, PC3M cells were incubated for 2 h with SPIO nanoparticles before investigating the presence of iron oxide nanoparticle in cells. As being shown in Figure 8(a), cells incubated with the targeting nanoparticles were stained in intensive blue color, indicating high cell uptake level of SPIO.

In comparison, the cells incubated with non-targeting nanoparticles (Figure 8(b)) or the control cells (Figure 8(c)) showed very weak blue appearance. These results confirmed that $scAb_{PSCA}$ functionalization was able to significantly increase the cell uptake of the magnetic nanoparticles in the PC3M cells.

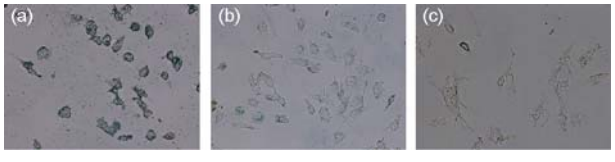

Figure 8 Prussian blue staining images (200×) of PC3M cells after 2 h incubation with $scAb_{PSCA}$-PEG-g-PEI-SPIO (a)or mPEG-g-PEI-SPIO (b)respectively at Fe concentration of 40 μg/mL in DMEM medium and normal PC3M cells (c) incubated with Prussian blue liquid for 30 min.

2.6 *In vitro* mri scan

SPIO as a MRI contrast agent internalized by cells in vitro was monitored by MRI (Figure 9).

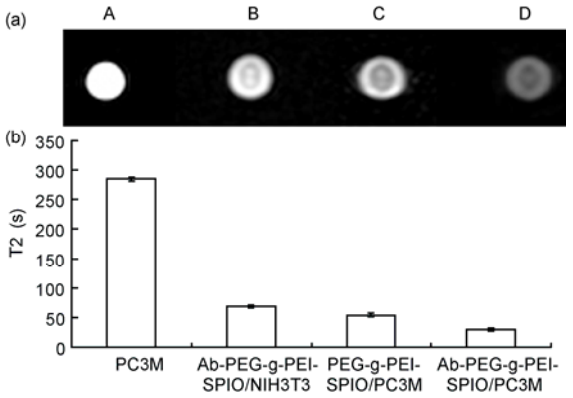

Figure 9 (a) T2-weighted MRI images of cells. (b) MRI T2 relaxation times of cells incubated with different nanoparticles. A: normal PC3M cells; B: NIH3T3 cells incubated with targeted SPIO; C: PC3M cells incubated with nontargeted SPIO; D: PC3M cells incubated with targeted SPIO, at same Fe concentration of 40 μg/mL.

The cells uptake level of SPIO correlates with the MRI signal intensity in T2-weighted images. Compared with the cells incubated with non-targeting nanoparticles or control cells, the MRI T2-weighted images of cells incubated with targeted nanoparticles appear to be much darker (at the same Fe concentration), and the T2 relaxation time is much shorter as well ($P<0.05$). These results indicate that $scAb_{PSCA}$-PEG-g-PEI-SPIO can bind to PC3M cells though PSCA receptor.

In this study we modified magnetic nanoparticles with PSCA scAb in a hope that the nanoparticles bearing this targeting ligand had specificity and high binding affinity to the target cells which could be non-invasively imaged by MRI. The results demonstrate that the targeting tropism of $scAb_{PSCA}$-PEG-g-PEI-SPIO to PCa cells, i.e. the MRI T2 signal intensity of PC3M cells was significantly decreased upon incubation with $scAb_{PSCA}$-PEG-g-PEI-SPIO, which is potentially in favor of getting ideal MRI image contrast.

Recently, as a non-invasive diagnostic method, MRI has been rapidly developed particularly in molecular MRI imaging applications. Connecting $scAb_{PSCA}$ with the contrast agent SPIO has been demonstrated to significantly enhance the MRI contrast in the targeted

PC3M. Noninvasive monitoring of the nanoparticle distribution, migration and metabolism is highly important for evaluating the therapeutic effect and safety of nanoparticulate system *in vivo*. Compared with the literature reports in which $scAb_{PSCA}$ were directly attached to SPIO, we used a polymeric vector bearing $scAb_{PSCA}$ to encapsulate SPIO. The nanosystem that we developed may not only enhance tumor MRI diagnosis, but also serve as a potential vehicle for nucleic acid delivery (i.e. gene or siRNA delivery). Actually, we have successfully complexed plasmid DNA and siRNA using this targeting vector in our laboratory, which has made the nucleic acid delivery vectors, possess the active targeting function to PCa and the MRI visibility in PCa gene therapy. The results will be reported elsewhere. It is expectable that we will achieve a more efficient MRI diagnosis for early stage cancer if we can mark the target cancer cell with more effective MRI contrast agent that can distinguish tumor tissues from healthy tissues *in vivo*. SPIO is a new MRI contrast agent mainly generating MRI T2 negative contrast effect. In comparison with other contrast agents, it has features including generating more signal change with commensurate iron, overcoming the drawback of low sensitivity for traditional MRI contrast agents, biodegradability, being recycled by normal cells through normal metabolic pathway, cell absorption easily observed using light microscope and electronmicroscope. In our experiment we embedded SPIO into the polymer carrier to form nanoparticles, and then conjugated the single-chain antibody to the external surface layer of the nanoparticles. With the antibody targeting and the T2 contrast negative effect of SPIO, the MRI imaging effect of PCa cells was significantly enhanced *in vitro*. Our results show the potential of $scAb_{PSCA}$-PEG-g-PEI-SPIO as a novel PCa MRI probe.

3 Conclusions

Taken together, in this study, we synthesized CDI-activated mPEG which was then grafted onto PEI. MRI T2 contrast agent SPIO nanoparticles were successfully complexed with PEG-g-PEI and a single antibody $scAb_{PSCA}$. These nanoparticles were then attached to the nanoparticles through PEG spacer to achieve a targeted delivery function in PCa cells. Our experiment results showed that PEG-g-PEI-SPIO has low toxicity, $scAb_{PSCA}$-PEG-g-PEI-SPIO had a higher transfection in PC3M. Additionally, this nanoparticle can effectively decrease the MRI T2 signal intensity of PCa cells leading to enhanced imaging effect. Thus, we achieved nanoprobe-based molecular targeting in PCa cells *in vitro*. Further work will be needed to test this MRI nanoprobe *in vivo* study.

We thank Dr. Chen WenJie for her kind assistance in antibody conjugation in this work.

1 Jemal A, Murray T, Ward E, et al. Cancer statistics. CA Cancer J Clin, 2005, 55: 10－30
2 Tannock I F, de Wit R, Berry W R, et al. Docetaxel plus prednisone or mitoxantrone plus prednisone for advanced prostate cancer. N Engl J Med, 2004, 351: 1502－1512
3 Men S, Cakar B, Conkbayir I, et al. Detection of prostatic carcinoma: the role of TRUS, TRUS guided biopsy, digital rectal examination, PSA and PSA density. J Exp Clin Cancer Res, 2001, 20: 473－480
4 Inahara M, Suzuki H, Kojima S, et al. Improved prostate cancer detection using systematic 14-core biopsy for large prostate glands with normal digital rectal examination findings. Urology, 2006, 68: 815－819
5 Gupta N P, Ansari M S, Dass S C. Transrectal ultrasound guided biopsy for detecting early prostate cancer: An Indian experience. Indian J Cancer, 2005, 42: 151－154
6 Wefer A E, Hricak H, Vigneron D B, et al. Sextant localization of prostate cancer: Comparison of sextant biopsy, magnetic resonance imaging and magnetic resonance spectroscopic imaging with step section histology. J Urol, 2000, 164: 400－404
7 Batllea C, Vilanova-Busquets J C, Saladie´-Roigc J M, et al. The value of endorectal MRI in the early diagnosis of prostate cancer. Eur Urol, 2003, 44: 201－208
8 Villers A, Puech P, Leroy X, et al. Dynamic contrast-enhanced MRI for preoperative identification of localised prostate cancer. European Urology Suppl, 2007, 6: 525－532
9 Pintaske J, Helms G, Bantleon R, et al. A preparation technique for quantitative investigation of SPIO-containing solutions and SPIO-labeled cells by MRI. Biomed Tech (Berl), 2005, 50: 174－180
10 Wagner S, Schnorr J, Pilgrimm H, et al. Monomer-coated very small superparamagnetic iron oxide particles as contrast medium for magnetic resonance imaging: Preclinical *in vivo* characterization. Invest Radiol, 2002, 37: 167－177
11 Okassa L N, Marchais H, Douziech-Eyrolles L, et al. Optimization of iron oxide nanoparticles encapsulation within poly(d,l-lactide-co-glycolide) sub-micron particles. Eur J Pharm Biopharm, 2007, 67: 31－38
12 Mohapatra S, Pramanik N, Ghosh S K, et al. Synthesis and characterization of ultrafine poly(vinylalcohol phosphate) coated magnetite nanoparticles. J Nanosci Nanotechnol, 2006, 6: 823－829
13 Fessi H. Preparation, characterization and surface study of poly-epsilon caprolactone magnetic microparticles. J Colloid Interface Sci, 2006, 300: 584－590

14 Liang S, Wang Y, Yu J, et al. Surface modified superparamagnetic iron oxide nanoparticles: As a new carrier for bio-magnetically targeted therapy. J Mater Sci Mater Med, 2007, 18: 2297－2302
15 Lee H, Lee E, Kim D K, et al. Antibiofouling polymer-coated superparamagnetic iron oxide nanoparticles as potential magnetic resonance contrast agents for *in vivo* cancer imaging. J Am Chem Soc, 2006, 128: 7383－7389
16 Tian H, Chen X, Lin H, et al. Micellization and reversible pH-senstive phase transfer of the hyperbranched multiarm PEI-PBLG copolymer. Chemistry, 2006, 12: 4305－4312
17 Kim J Y, Lee J E, Lee S H, et al. Designed fabrication of multifunctional polymer nanomedical platform for simultaneous cancer-targeted imaging and magnetically-guided drug delivery. Adv Mater, 2008, 20: 478－483
18 Boutry S, Laurent S, Elst L V, et al. Specific E-selectin targeting with a superparamagnetic MRI contrast agent. Contrast Media Mol Imaging, 2006, 1: 15－22
19 Liang S, Wang Y, Yu J, et al. Surface modified superparamagnetic iron oxide nanoparticles: As a new carrier for bio-magnetically targeted therapy. J Mater Sci Mater Med, 2007, 18: 2297－2302
20 Li Y, Xu X, Deng C, et al. Immobilization of trypsin on superparamagnetic nanoparticles for rapid and effective proteolysis. J Proteome Res, 2007, 6: 3849－3855
21 Park I K, Ng C P, Wang J, et al. Determination of nanoparticle vehicle unpackaging by MR imaging of a T(2) magnetic relaxation switch. Biomaterials, 2008, 29: 724－732
22 Gupta A K, Gupta M. Synthesis and surface engineering of iron oxide nanopartides for biomedical applications. Biomaterials, 2005, 26: 3995－4021
23 Lam J S, Yamashiro J, Shintaku I P, et al. Prostate stem cell antigen is overexpressed in prostate cancer metastases. Clin Cancer Res, 2005, 11: 2591－2596
24 Morgenroth A, Cartellieri M, Schmitz M, et al. Targeting of tumor cells expressing the prostate stem cell antigen (PSCA) using genetically engineered T-Cells. Prostate, 2007, 67: 1121－1131
25 Garcia-Hernandez Mde L, Gray A, Hubby B, et al. Prostate stem cell antigen vaccination induces a long-term protective immune response against prostate cancer in the absence of autoimmunity. Cancer Res, 2008, 68: 861－869
26 Sun S, Zeng H, Robinson D B, et al. Monodisperse MFe_2O_4(M = Fe, Co, Mn) nanoparticles. J Am Chem Soc, 2004, 126: 273－279
27 Tromsdorf U I, Bigall N C, Kaul M G, et al. Size and surface effects on the MRI relaxivity of manganese ferrite nanoparticle contrast agents. Nano Lett, 2007, 7: 2422－2427
28 Shen X M. N-maleimidly Polymer Derivatives. US Patent, US0013797 A1, 2006-01-19
29 Shuai X, Merdan T, Unger F, et al. Novel biodegradable ternary copolymers hy-PEI-g-PCL-b-PEG: Synthesis, characterization, and potential as efficient nonviral gene delivery vectors. Macromolecules, 2003, 36: 5751－5759
30 Greg T H. Bioconjugate Techniques. New York: Academic Press, 1996. 463－464
31 Kuhn D M, Balkis M, Chandra J, et al. Uses and limitations of the XTT assay in studies of Candida growth and metabolism. J Clin Microbiol, 2003, 41: 506－508